

## Observation of $D^+ \rightarrow \eta e^+ \nu_e$

R. E. Mitchell,<sup>1</sup> M. R. Shepherd,<sup>1</sup> D. Besson,<sup>2</sup> T. K. Pedlar,<sup>3</sup> D. Cronin-Hennessy,<sup>4</sup>  
 K. Y. Gao,<sup>4</sup> J. Hietala,<sup>4</sup> Y. Kubota,<sup>4</sup> T. Klein,<sup>4</sup> B. W. Lang,<sup>4</sup> R. Poling,<sup>4</sup> A. W. Scott,<sup>4</sup>  
 A. Smith,<sup>4</sup> P. Zweber,<sup>4</sup> S. Dobbs,<sup>5</sup> Z. Metreveli,<sup>5</sup> K. K. Seth,<sup>5</sup> A. Tomaradze,<sup>5</sup>  
 J. Ernst,<sup>6</sup> K. M. Ecklund,<sup>7</sup> H. Severini,<sup>8</sup> W. Love,<sup>9</sup> V. Savinov,<sup>9</sup> O. Aquines,<sup>10</sup>  
 A. Lopez,<sup>10</sup> S. Mehrabyan,<sup>10</sup> H. Mendez,<sup>10</sup> J. Ramirez,<sup>10</sup> G. S. Huang,<sup>11</sup> D. H. Miller,<sup>11</sup>  
 V. Pavlunin,<sup>11</sup> B. Sanghi,<sup>11</sup> I. P. J. Shipsey,<sup>11</sup> B. Xin,<sup>11</sup> G. S. Adams,<sup>12</sup> M. Anderson,<sup>12</sup>  
 J. P. Cummings,<sup>12</sup> I. Danko,<sup>12</sup> D. Hu,<sup>12</sup> B. Moziak,<sup>12</sup> J. Napolitano,<sup>12</sup> Q. He,<sup>13</sup> J. Insler,<sup>13</sup>  
 H. Muramatsu,<sup>13</sup> C. S. Park,<sup>13</sup> E. H. Thorndike,<sup>13</sup> F. Yang,<sup>13</sup> M. Artuso,<sup>14</sup> S. Blusk,<sup>14</sup>  
 J. Butt,<sup>14</sup> J. Li,<sup>14</sup> N. Mena,<sup>14</sup> R. Mountain,<sup>14</sup> S. Nisar,<sup>14</sup> K. Randrianarivony,<sup>14</sup>  
 R. Sia,<sup>14</sup> T. Skwarnicki,<sup>14</sup> S. Stone,<sup>14</sup> J. C. Wang,<sup>14</sup> K. Zhang,<sup>14</sup> G. Bonvicini,<sup>15</sup>  
 D. Cinabro,<sup>15</sup> M. Dubrovin,<sup>15</sup> A. Lincoln,<sup>15</sup> D. M. Asner,<sup>16</sup> K. W. Edwards,<sup>16</sup> P. Naik,<sup>16</sup>  
 R. A. Briere,<sup>17</sup> T. Ferguson,<sup>17</sup> G. Tatishvili,<sup>17</sup> H. Vogel,<sup>17</sup> M. E. Watkins,<sup>17</sup> J. L. Rosner,<sup>18</sup>  
 N. E. Adam,<sup>19</sup> J. P. Alexander,<sup>19</sup> D. G. Cassel,<sup>19</sup> J. E. Duboscq,<sup>19</sup> R. Ehrlich,<sup>19</sup>  
 L. Fields,<sup>19</sup> R. S. Galik,<sup>19</sup> L. Gibbons,<sup>19</sup> R. Gray,<sup>19</sup> S. W. Gray,<sup>19</sup> D. L. Hartill,<sup>19</sup>  
 B. K. Heltsley,<sup>19</sup> D. Hertz,<sup>19</sup> C. D. Jones,<sup>19</sup> J. Kandaswamy,<sup>19</sup> D. L. Kreinick,<sup>19</sup>  
 V. E. Kuznetsov,<sup>19</sup> H. Mahlke-Krüger,<sup>19</sup> D. Mohapatra,<sup>19</sup> P. U. E. Onyisi,<sup>19</sup>  
 J. R. Patterson,<sup>19</sup> D. Peterson,<sup>19</sup> J. Pivarski,<sup>19</sup> D. Riley,<sup>19</sup> A. Ryd,<sup>19</sup> A. J. Sadoff,<sup>19</sup>  
 H. Schwarthoff,<sup>19</sup> X. Shi,<sup>19</sup> S. Stroiney,<sup>19</sup> W. M. Sun,<sup>19</sup> T. Wilksen,<sup>19</sup> S. B. Athar,<sup>20</sup>  
 R. Patel,<sup>20</sup> V. Potlia,<sup>20</sup> J. Yelton,<sup>20</sup> P. Rubin,<sup>21</sup> C. Cawfield,<sup>22</sup> B. I. Eisenstein,<sup>22</sup>  
 I. Karliner,<sup>22</sup> D. Kim,<sup>22</sup> N. Lowrey,<sup>22</sup> M. Selen,<sup>22</sup> E. J. White,<sup>22</sup> and J. Wiss<sup>22</sup>

(CLEO Collaboration)

<sup>1</sup>*Indiana University, Bloomington, Indiana 47405*

<sup>2</sup>*University of Kansas, Lawrence, Kansas 66045*

<sup>3</sup>*Luther College, Decorah, Iowa 52101*

<sup>4</sup>*University of Minnesota, Minneapolis, Minnesota 55455*

<sup>5</sup>*Northwestern University, Evanston, Illinois 60208*

<sup>6</sup>*State University of New York at Albany, Albany, New York 12222*

<sup>7</sup>*State University of New York at Buffalo, Buffalo, New York 14260*

<sup>8</sup>*University of Oklahoma, Norman, Oklahoma 73019*

<sup>9</sup>*University of Pittsburgh, Pittsburgh, Pennsylvania 15260*

<sup>10</sup>*University of Puerto Rico, Mayaguez, Puerto Rico 00681*

<sup>11</sup>*Purdue University, West Lafayette, Indiana 47907*

<sup>12</sup>*Rensselaer Polytechnic Institute, Troy, New York 12180*

<sup>13</sup>*University of Rochester, Rochester, New York 14627*

<sup>14</sup>*Syracuse University, Syracuse, New York 13244*

<sup>15</sup>*Wayne State University, Detroit, Michigan 48202*

<sup>16</sup>*Carleton University, Ottawa, Ontario, Canada K1S 5B6*

<sup>17</sup>*Carnegie Mellon University, Pittsburgh, Pennsylvania 15213*

<sup>18</sup>*Enrico Fermi Institute, University of Chicago, Chicago, Illinois 60637*

<sup>19</sup>*Cornell University, Ithaca, New York 14853*

<sup>20</sup>*University of Florida, Gainesville, Florida 32611*

<sup>21</sup>*George Mason University, Fairfax, Virginia 22030*

<sup>22</sup>*University of Illinois, Urbana-Champaign, Illinois 61801*

(Dated: February 28, 2008)

## Abstract

Using a  $281 \text{ pb}^{-1}$  data sample collected at the  $\psi(3770)$  resonance with the CLEO-c detector at the Cornell Electron Storage Ring, we report the first observation of  $D^+ \rightarrow \eta e^+ \nu_e$ . We also set upper limits for  $D^+ \rightarrow \eta' e^+ \nu_e$  and  $D^+ \rightarrow \phi e^+ \nu_e$  that are about two orders of magnitude more restrictive than those obtained by previous experiments.

The quark mixing parameters are fundamental constants of the Standard Model (SM) of particle physics. They determine the nine weak-current quark coupling elements of the Cabibbo-Kobayashi-Maskawa (CKM) matrix [1]. Charm semileptonic decays have been studied in considerable detail because they provide direct measurements of the magnitudes of the CKM elements  $V_{cd}$  and  $V_{cs}$ , and a stringent test of theoretical predictions of strong interaction effects in the decay amplitude. In order to gain a complete understanding of charm semileptonic decays it is important to study as many exclusive modes as possible. Several rare modes have yet to be observed.

The most precise measurements to date of absolute branching fractions of  $D$ -meson semileptonic decays have been made by CLEO-c at the  $\psi(3770)$  [2–5]. Absolute exclusive semileptonic branching fractions were measured for nine final states that included a single  $K$ ,  $\pi$ ,  $K^*$ ,  $\rho$ , or  $\omega$  meson. Summing the exclusive semileptonic branching fractions gives  $\sum \mathcal{B}(D_{\text{excl}}^0) = [6.3 \pm 0.2(\text{stat}) \pm 0.2(\text{syst})]\%$  and  $\sum \mathcal{B}(D_{\text{excl}}^+) = [15.2 \pm 0.3(\text{stat}) \pm 0.4(\text{syst})]\%$ . CLEO has also measured the absolute branching fractions of inclusive semileptonic decays and found  $\mathcal{B}(D^0 \rightarrow Xe^+\nu_e) = (6.46 \pm 0.17 \pm 0.13)\%$  and  $\mathcal{B}(D^+ \rightarrow Xe^+\nu_e) = (16.13 \pm 0.20 \pm 0.33)\%$  [6]. These measurements are consistent with, but larger than, the sum of the exclusive semileptonic branching fractions. Although the possibility of additional semileptonic modes of the  $D^0$  and  $D^+$  with large branching fractions is excluded, a window for additional semileptonic decay modes remains.

Semileptonic decays of a  $D$  meson with an  $\eta$  or  $\eta'$  in the final state have not yet been observed. Their discovery would open future opportunities to obtain information about  $\eta - \eta'$  mixing [7]. They also probe the composition of the  $\eta$  and  $\eta'$  wave functions when combined with measurements of the corresponding  $D_s$  semileptonic decays [8] and gauge the possible role of weak annihilation in the corresponding  $D_s$ -meson semileptonic decays [8]. The process  $D^+ \rightarrow \phi e^+\nu_e$  is not expected to occur in the absence of mixing between the  $\omega$  and  $\phi$  [9].

We report herein the first observation and absolute branching fraction measurement of  $D^+ \rightarrow \eta e^+\nu_e$ , and results of searches for  $D^+ \rightarrow \eta' e^+\nu_e$  and  $D^+ \rightarrow \phi e^+\nu_e$ . (Throughout this Letter charge-conjugate modes are implied.) The data sample used for these measurements consists of an integrated luminosity of  $281 \text{ pb}^{-1}$  at the  $\psi(3770)$  resonance, and includes about  $8 \times 10^5 D^+D^-$  events [10]. The data were produced in  $e^+e^-$  collisions at the Cornell Electron Storage Ring (CESR-c) and collected with the CLEO-c detector. This is the same data set used in Refs. [4–6, 10].

CLEO-c is a general-purpose solenoidal detector. The charged particle tracking system covers a solid angle of 93% of  $4\pi$  and consists of a small-radius six-layer low mass stereo wire drift chamber concentric with, and surrounded by, a 47-layer cylindrical drift chamber. The chambers operate in a 1.0 T magnetic field and achieve a momentum resolution of  $\sim 0.6\%$  at  $p = 1 \text{ GeV}/c$ . The main drift chamber provides specific-ionization ( $dE/dx$ ) measurements that discriminate between charged pions and kaons. Additional hadron identification is provided by a Ring-Imaging Cherenkov (RICH) detector covering approximately 80% of  $4\pi$ . Identification of positrons and detection of neutral pions and eta mesons relies on an electromagnetic calorimeter consisting of 7800 cesium iodide crystals and covering about 93% of  $4\pi$ . The calorimeter achieves a photon energy resolution of 2.2% at  $E_\gamma = 1 \text{ GeV}$  and 5% at 100 MeV. The CLEO-c detector is described in detail elsewhere [11].

The technique for our analysis was first applied by the Mark III collaboration [12] at SPEAR. The presence of two  $D^\pm$  mesons in a  $D^+D^-$  event allows a tag sample to be defined in which a  $D^-$  is reconstructed in a hadronic decay mode. A sub-sample is then defined in

which a positron and a set of hadrons, as a signature of a semileptonic decay, are required in addition to the tag. The tag yield can be expressed as  $N_{\text{tag}} = 2N_{DD}\mathcal{B}_{\text{tag}}\epsilon_{\text{tag}}$ , where  $N_{DD}$  is the produced number of  $D^+D^-$  pairs,  $\mathcal{B}_{\text{tag}}$  is the branching fraction of hadronic modes used in the tag sample, and  $\epsilon_{\text{tag}}$  is the tag efficiency. The yield of tags with a semileptonic decay can be expressed as  $N_{\text{tag,SL}} = 2N_{DD}\mathcal{B}_{\text{tag}}\mathcal{B}_{\text{SL}}\epsilon_{\text{tag,SL}}$  where  $\mathcal{B}_{\text{SL}}$  is the semileptonic decay branching fraction, including subsidiary branching fractions, and  $\epsilon_{\text{tag,SL}}$  is the efficiency of finding the tag and the semileptonic decay in the same event. From the expressions for  $N_{\text{tag}}$  and  $N_{\text{tag,SL}}$  we obtain

$$\mathcal{B}_{\text{SL}} = \frac{N_{\text{tag,SL}}}{N_{\text{tag}}} \frac{\epsilon_{\text{tag}}}{\epsilon_{\text{tag,SL}}} = \frac{N_{\text{tag,SL}}/\epsilon}{N_{\text{tag}}}, \quad (1)$$

where  $\epsilon = \epsilon_{\text{tag,SL}}/\epsilon_{\text{tag}}$  is the effective signal efficiency. The branching fraction determined by tagging is an absolute measurement. It is independent of the integrated luminosity and number of  $D^+$  mesons in the data sample. Due to the large solid angle acceptance and high segmentation of the CLEO-c detector and the low multiplicity of the events  $\epsilon_{\text{tag,SL}} \approx \epsilon_{\text{tag}}\epsilon_{\text{SL}}$ , where  $\epsilon_{\text{SL}}$  is the semileptonic decay efficiency. Hence the ratio  $\epsilon_{\text{tag,SL}}/\epsilon_{\text{tag}}$  is insensitive to most systematic effects associated with the tag mode and the absolute branching fraction determined with this procedure is nearly independent of the tag mode.

Candidate events are selected by reconstructing a  $D^-$  tag in one of the following six hadronic final states:  $K_S^0\pi^-$ ,  $K^+\pi^-\pi^-$ ,  $K_S^0\pi^-\pi^0$ ,  $K^+\pi^-\pi^-\pi^0$ ,  $K_S^0\pi^-\pi^-\pi^+$ , and  $K^+K^-\pi^-$ . Tagged events are selected based on two variables:  $\Delta E \equiv E_D - E_{\text{beam}}$ , the difference between the energy of the  $D^-$  tag candidate ( $E_D$ ) and the beam energy ( $E_{\text{beam}}$ ), and the beam-constrained mass  $M_{\text{bc}} \equiv \sqrt{E_{\text{beam}}^2/c^4 - |\vec{p}_D|^2/c^2}$ , where  $\vec{p}_D$  is the measured momentum of the  $D^-$  candidate. Selection criteria for tracks,  $\pi^0$  and  $K_S^0$  candidates used in the reconstruction of tags are described in Ref. [13]. If multiple candidates are present in the same tag mode, one candidate per tag charge with the smallest  $\Delta E$  is chosen. The yield of each tag mode, and the combined yield of all six tag modes, are obtained from fits to the  $M_{\text{bc}}$  distributions, where the signal shape includes the effects of beam energy smearing, initial state radiation, the line shape of the  $\psi(3770)$ , and reconstruction resolution, and the background is described by an ARGUS function [14], which models combinatorial contributions. The data sample comprises approximately 163,000 reconstructed charged tags (Table I).

TABLE I: Tag yields of the six  $D^-$  hadronic modes with statistical uncertainties.

Tag Mode	$N_{\text{tag}}$
$D^- \rightarrow K_S^0\pi^-$	11469 $\pm$ 116
$D^- \rightarrow K^+\pi^-\pi^-$	79933 $\pm$ 293
$D^- \rightarrow K_S^0\pi^-\pi^0$	25243 $\pm$ 212
$D^- \rightarrow K^+\pi^-\pi^-\pi^0$	23733 $\pm$ 185
$D^- \rightarrow K_S^0\pi^-\pi^-\pi^+$	16446 $\pm$ 177
$D^- \rightarrow K^-K^+\pi^-$	6785 $\pm$ 97
All Tags	163057 $\pm$ 483

After a tag is identified, we search for a positron and a set of hadrons recoiling against the tag. (Muons are not used because the CLEO-c muon identification system has poor acceptance in the momentum range characteristic of semileptonic  $D$  decays at the  $\psi(3770)$ .)

Positron candidates are selected based on a likelihood ratio constructed from three inputs: the ratio of the energy deposited in the calorimeter to the measured momentum ( $E/p$ ),  $dE/dx$ , and RICH information [3]. Furthermore, candidates must have momenta of at least 200 MeV/ $c$  and satisfy  $|\cos\theta| < 0.90$ , where  $\theta$  is the angle between the positron direction and the beam axis. The efficiency for positron identification has been measured primarily with radiative Bhabha events. In the kinematic region used in this analysis, the efficiency rises from about 50% at 200 MeV/ $c$  to 95% just above 300 MeV/ $c$  and is roughly constant thereafter. The rates for misidentifying charged pions and kaons as positrons, averaged over the momentum range, is approximately 0.1%. Bremsstrahlung photons are recovered by adding showers within  $5^\circ$  of the positron that are not matched to other particles.

Hadronic tracks produced in semileptonic  $D^+$  decay are required to have momenta above 50 MeV/ $c$  and  $|\cos\theta| < 0.93$ . Pion and kaon candidates are required to have  $dE/dx$  measurements within three standard deviations ( $3\sigma$ ) of the expected value. For tracks with momenta greater than 700 MeV/ $c$ , RICH information, if available, is combined with  $dE/dx$ . The efficiencies (95% or higher) and misidentification rates (a few per cent) are determined with charged pion and kaon samples from hadronic  $D$  decays.

We select  $\pi^0$  candidates from pairs of photons, each having an energy of at least 30 MeV, and a shower shape consistent with that expected for a photon. A kinematic fit is performed constraining the invariant mass of the photon pair to the known  $\pi^0$  mass. The candidate is accepted if the unconstrained invariant mass is within  $3\sigma$  of the nominal  $\pi^0$  mass, where  $\sigma$  (typically 6 MeV/ $c^2$ ) is determined for that candidate from the kinematic fit, and the kinematic parameters for the  $\pi^0$  determined with the fit are used in further reconstruction. We reconstruct  $\eta$  candidates in two decay modes. For the decay  $\eta \rightarrow \gamma\gamma$ , candidates are formed using the same procedure as for  $\pi^0$  except that  $\sigma \sim 12$  MeV/ $c^2$ . For  $\eta \rightarrow \pi^+\pi^-\pi^0$  we require that the invariant mass of the three pions be within 12 MeV/ $c^2$  of the known  $\eta$  mass. We reconstruct  $\eta'$  in the decay mode  $\eta' \rightarrow \pi^+\pi^-\eta$ . We require  $|m_{\pi^+\pi^-\eta} - m_{\eta'}| < 10$  MeV/ $c^2$ . We reconstruct  $\phi$  candidates in the mode  $\phi \rightarrow K^+K^-$  requiring  $|m_{KK} - m_\phi| < 13.5$  MeV/ $c^2$ . For both the  $\eta'$  and  $\phi$  these mass cuts correspond to  $\pm 3\sigma$ .

The  $D^-$  tag and  $D^+$  semileptonic decay are combined if they account for all tracks in the event. Semileptonic decays are identified with  $U \equiv E_{\text{miss}} - c|\vec{p}_{\text{miss}}|$ , where  $E_{\text{miss}}$  and  $\vec{p}_{\text{miss}}$  are the missing energy and momentum of the  $D^+$  meson. If the decay products have been correctly identified,  $U$  is expected to be zero, since only a neutrino is undetected. The resolution in  $U$  is improved by constraining the magnitude and direction of the  $D^+$  momentum to be  $p_{D^+} = \sqrt{E_{\text{beam}}^2/c^2 - c^2m_D^2}$ , and  $\vec{p}_{D^+} = -\vec{p}_{D^-}$  [3], respectively. Due to the finite resolution of the detector, the distribution in  $U$  is approximately Gaussian, centered at  $U = 0$  with  $\sigma \sim 10$  MeV (the width varies by mode). The number of events with multiple candidates varies by mode, ranging from zero for  $D^+ \rightarrow \phi e^+\nu_e$  to 83% for  $D^+ \rightarrow \eta'(\pi^+\pi^-\eta)e^+\nu_e$ . To remove multiple candidates in each semileptonic mode one combination is chosen per tag mode per tag charge, based on the proximity of the invariant masses of the  $\pi^0$ ,  $\eta$ ,  $\eta'$ , or  $\phi$  candidates to their expected masses.

The  $U$  distributions for  $D^+ \rightarrow \eta e^+\nu_e$  for each  $\eta$  decay mode with all tag modes combined are shown in Fig. 1. The  $U$  distributions in data for  $D^+ \rightarrow \eta'(\pi^+\pi^-\eta)e^+\nu_e$  and  $D^+ \rightarrow \phi(K^+K^-)e^+\nu_e$  have no entries in  $-250 < U < 250$  MeV and are not included in Fig. 1 [15]. The yield for  $D^+ \rightarrow \eta e^+\nu_e$  is determined from a binned likelihood fit to the  $U$  distribution where the signal is described by a modified Crystal Ball function with two power-law tails [16] which account for initial- and final-state radiation (FSR) and mismeasured tracks. The signal parameters are fixed with a GEANT-based Monte Carlo (MC) simulation [17] in

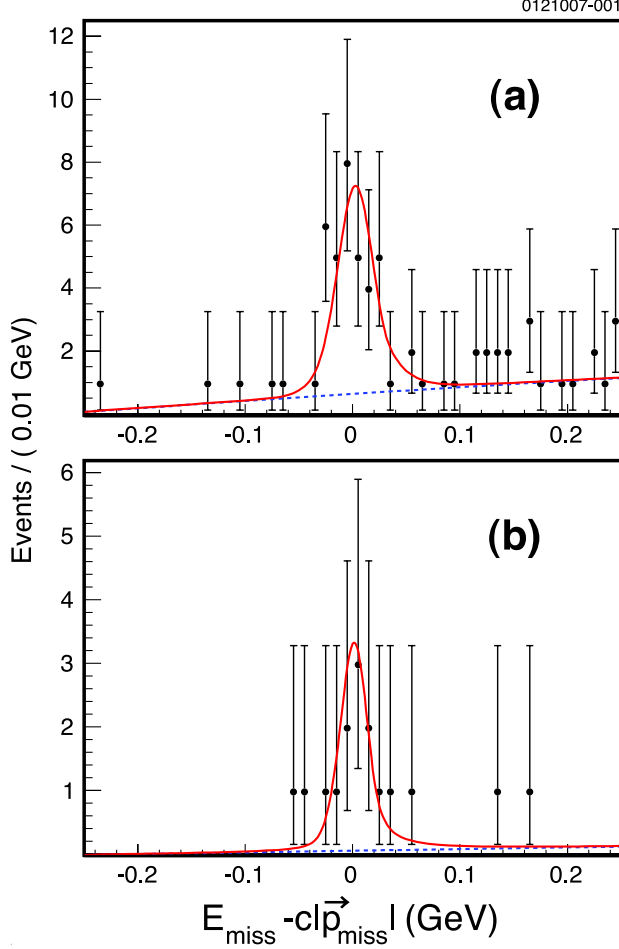


FIG. 1: Fits to the  $U$  distributions in data (filled circles with error bars) for  $D^+ \rightarrow \eta e^+ \nu_e$  for two  $\eta$  decay modes: (a)  $\eta \rightarrow \gamma\gamma$ , (b)  $\eta \rightarrow \pi^+ \pi^- \pi^0$ . The solid line represents the fit of the sum of the signal function and background function to the data. The dashed line indicates the background contribution.

fits to the data. The background functions are determined by a simulation that incorporates all available data on  $D$  meson decays. The backgrounds are small and arise mostly from misreconstructed semileptonic decays with correctly reconstructed tags. For  $D^+ \rightarrow \eta(\gamma\gamma)e^+ \nu_e$ , there is background from  $D^+ \rightarrow K_S^0(\pi^0\pi^0)e^+ \nu_e$  and  $D^+ \rightarrow \pi^0 e^+ \nu_e$ . The background shape parameters are fixed, while the background normalizations are allowed to float in fits to the data. The signal yields  $N_{\text{tag,SL}}$  are given in Table II. The fits describe the data well. After increasing the backgrounds by one statistical  $\sigma$ , the probabilities that background fluctuations account for the signals are  $2 \times 10^{-10}$  and  $6 \times 10^{-8}$ , corresponding to  $6.3\sigma$  and  $5.3\sigma$ , for  $D^+ \rightarrow \eta(\gamma\gamma)e^+ \nu_e$  and  $D^+ \rightarrow \eta(\pi^+ \pi^- \pi^0)e^+ \nu_e$ , respectively. This is the first observation of  $D^+ \rightarrow \eta e^+ \nu_e$ .

The absolute branching fractions and 90% confidence level (C.L.) upper limits in Table II are obtained from Eq. (1). The signal efficiencies,  $\epsilon$ , are determined by MC simulation, and have been weighted by the tag yields shown in Table I. Due to differences between the simulation and data, corrections are applied to  $N_{\text{tag,SL}}$  for  $\pi^0$  and  $\eta$  finding, positron identification, and charged  $\pi$  and  $K$  identification. The corrections are given in Table III.

We consider the following sources of systematic uncertainty and give our estimates of their magnitudes in Table III. Where these estimates vary by decay mode a range is given. The uncertainty in the track finding efficiency is estimated with missing mass techniques applied to the data and simulation [10]. The correction to the  $\pi^0 \rightarrow \gamma\gamma$  ( $\eta \rightarrow \gamma\gamma$ ) detection efficiency and its uncertainty are estimated with the same method. The momentum-dependent correction to the positron identification, and its uncertainty, are obtained from comparisons of the detector response to positrons from radiative Bhabhas in data and MC simulations [3]. The corrections to the charged pion and kaon identification efficiencies, and the associated uncertainties, are estimated using hadronic  $D$ -meson decays. The uncertainty in the number of tags is estimated by using alternative signal functions in the fits, and by counting. The uncertainty in modelling the background shapes in the fits to the  $U$  distributions has contributions from the uncertainties in the simulation of the positron and hadron fake rates. The uncertainty associated with the requirement that there be no additional tracks in tagged semileptonic events is estimated by comparing fully reconstructed  $D\bar{D}$  events in data and simulation. The uncertainty associated with the shape of the signal function is estimated by using alternative signal functions. The uncertainty in the semileptonic reconstruction efficiencies due to imperfect knowledge of the semileptonic form factors is estimated by varying the form factors in the corresponding well-studied transitions  $D \rightarrow K/\pi/K^*e^+\nu_e$ , by their uncertainties and assuming that the resulting changes in efficiency are a measure of the uncertainty in efficiencies for the semileptonic transitions being studied here [2]. The uncertainty associated with the simulation of FSR and bremsstrahlung in the detector material is estimated by varying the amount of FSR modelled by the PHOTOS algorithm [18] and by repeating the analysis with and without recovery of FSR photons. The uncertainty associated with the simulation of initial-state radiation ( $e^+e^- \rightarrow D\bar{D}\gamma$ ) is negligible. These estimates are added in quadrature to obtain the total systematic uncertainties reported in Table II.

For the upper limits in Table II, systematic uncertainties are incorporated by combining with statistical uncertainties in quadrature and increasing the upper limit on the number of observed events by one  $\sigma$  of the combined uncertainty. Systematic uncertainties for all modes are much smaller than statistical uncertainties.

Our branching fractions for  $D^+ \rightarrow \eta e^+\nu_e$  and upper limits for  $D^+ \rightarrow \eta' e^+\nu_e$  and  $D^+ \rightarrow \phi e^+\nu_e$  are compared to previous upper limits [9] in Table. II. The branching fractions measured using the two  $\eta$  decay modes are consistent, and the combined branching fraction is consistent with the PDG upper limit. Theoretical predictions for  $\mathcal{B}(D^+ \rightarrow \eta e^+\nu_e)$  and  $\mathcal{B}(D^+ \rightarrow \eta' e^+\nu_e)$  in the ISGW2 model [7] and a model (FK) which combines heavy-quark symmetry and properties of the chiral Lagrangian [19], are also listed in Table. II. Our  $\mathcal{B}(D^+ \rightarrow \eta e^+\nu_e)$  is consistent with these predictions, although our statistical uncertainty is large. The upper limits for  $D^+ \rightarrow \eta' e^+\nu_e$  and  $D^+ \rightarrow \phi e^+\nu_e$  are about two orders of magnitude more restrictive than previous experimental limits.

In summary, we have made the first observation of  $D^+ \rightarrow \eta e^+\nu_e$  and measured the branching fraction, which is found to be consistent with model predictions. The sum of exclusive semileptonic branching fractions of the  $D^+$  is approximately 0.9% smaller than the measured inclusive semileptonic branching fraction. Our  $\mathcal{B}(D^+ \rightarrow \eta e^+\nu_e)$  increases the exclusive sum by about 0.1%, indicating that further exclusive rare semileptonic modes may await discovery. We have searched for the decays  $D^+ \rightarrow \eta' e^+\nu_e$  and  $D^+ \rightarrow \phi e^+\nu_e$  and set significantly improved upper limits for each mode. The predictions for  $\mathcal{B}(D^+ \rightarrow \eta' e^+\nu_e)$  [7, 19] are similar in magnitude to our upper limit. If these models are correct, an

observation of  $D^+ \rightarrow \eta' e^+ \nu_e$  is likely in the near future.

We gratefully acknowledge the effort of the CESR staff in providing us with excellent luminosity and running conditions. This work was supported by the A.P. Sloan Foundation, the National Science Foundation, the U.S. Department of Energy, and the Natural Sciences and Engineering Research Council of Canada.

- 
- [1] M. Kobayashi and T. Maskawa, *Theor. Phys.* **49**, 652 (1973).
  - [2] G.S. Huang *et al.* [CLEO Collaboration], *Phys. Rev. Lett.* **95**, 181801 (2005).
  - [3] T.E. Coan *et al.* [CLEO Collaboration], *Phys. Rev. Lett.* **95**, 181802 (2005).
  - [4] D. Cronin-Hennessey *et al.*, [CLEO Collaboration], *Phys. Rev. Lett.* **100**, 251802 (2008), and S. Dobbs *et al.*, [CLEO Collaboration], *Phys. Rev. D* **77**, 112005 (2008).
  - [5] J. Y. Ge *et al.*, [CLEO Collaboration], arXiv:0810.3878 submitted to *Phys. Rev. D* (2008).
  - [6] N.E. Adam *et al.* [CLEO Collaboration], *Phys. Rev. Lett.* **97**, 251801 (2006).
  - [7] D. Scora and N. Isgur, *Phys. Rev. D* **52**, 2783 (1995).
  - [8] S. Bianco, F. Fabbri, D. Benson, and I. Bigi, *La Rivista del Nuovo Cimento*, 26, **7-8** (2003).
  - [9] W.-M. Yao *et al.* [Particle Data Group], *J. Phys. G* **33**, 1 (2006).
  - [10] S. Dobbs *et al.* [CLEO Collaboration], *Phys. Rev. D* **76**, 112001 (2007).
  - [11] Y. Kubota *et al.*, *Nucl. Instrum. Meth. Phys. Res., Sect. A* **320**, 66 (1992); D. Peterson *et al.*, *Nucl. Instrum. Meth. Phys. Res., Sect. A* **478**, 142 (2002); M. Artuso *et al.*, *Nucl. Instrum. Meth. Phys. Res., Sect. A* **554**, 147 (2005).
  - [12] J. Adler *et al.* [Mark III Collaboration], *Phys. Rev. Lett.* **62**, 1821 (1989).
  - [13] Q. He *et al.* [CLEO Collaboration], *Phys. Rev. Lett.* **95**, 121801 (2005).
  - [14] H. Albrecht *et al.*, [ARGUS Collaboration], *Phys. Lett. B* **241**, 278 (1990).
  - [15] We have also searched for  $D^+ \rightarrow \eta' e^+ \nu_e$  with  $\eta' \rightarrow \rho^0 \gamma$ . This mode has a large branching fraction and detection efficiency but also large background. No significant signal was observed. Uncertainties in the simulation of the background complicate extraction of an upper limit and so this mode is not used.
  - [16] T. Skwarnicki, Ph.D thesis, Jagiellonian University in Krakow, 1986, DESY Report No. F31-86-02.
  - [17] R. Brun *et al.*, **GEANT 3.21**, CERN Program Library Long Writeup W5013, unpublished.
  - [18] E. Barberio and Z. Was, *Comput. Phys. Commun.* **79**, 291 (1994).
  - [19] S. Fajfer and J. Kamenik, *Phys. Rev. D* **71**, 014020 (2005).

TABLE II: Signal efficiencies, yields (90% C.L. intervals), and branching fractions (90% C.L. upper limits) for  $D^+ \rightarrow \eta' e^+ \nu_e$ , ( $D^+ \rightarrow \eta' e^+ \nu_e$  and  $\phi e^+ \nu_e$ ) in units of  $\times 10^{-4}$  in this work and comparisons to PDG [9] and two theoretical predictions ISGWII [7] and FK [19]. In the fourth column the first uncertainty is statistical and the second systematic. In other columns the uncertainty is statistical or statistical and systematic combined in quadrature. The efficiencies include subsidiary branching fractions from PDG [9].

Decay Mode	$\epsilon$ (%)	$N_{\text{tag, SL}}$	$\mathcal{B}_{\text{SL}}$	$\mathcal{B}_{\text{SL}}$ (PDG)	$\mathcal{B}_{\text{SL}}$ (ISGWII)	$\mathcal{B}_{\text{SL}}$ (FK)
$D^+ \rightarrow \eta(\gamma\gamma) e^+ \nu_e$	$15.13 \pm 0.07$	$32.6 \pm 6.7$	$13.2 \pm 2.3 \pm 0.6$			
$D^+ \rightarrow \eta(\pi^+ \pi^- \pi^0) e^+ \nu_e$	$5.99 \pm 0.04$	$13.3 \pm 4.0$	$13.6 \pm 3.7 \pm 0.5$			
$D^+ \rightarrow \eta e^+ \nu_e$ (Combined)			$13.3 \pm 2.0 \pm 0.6$	$<70$	11	10
$D^+ \rightarrow \eta'(\pi^+ \pi^- \eta \rightarrow \pi^+ \pi^- \gamma\gamma) e^+ \nu_e$	$3.38 \pm 0.02$	$(0.00, 2.30)$	$<4.4$			
$D^+ \rightarrow \eta'(\pi^+ \pi^- \eta \rightarrow 2(\pi^+ \pi^-) \pi^0) e^+ \nu_e$	$0.85 \pm 0.01$	$(0.00, 2.30)$	$<17.3$			
$D^+ \rightarrow \eta' e^+ \nu_e$ (Combined)	$4.23 \pm 0.02$	$(0.00, 2.30)$	$<3.5$	$<110$	5	1.6
$D^+ \rightarrow \phi(K^+ K^-) e^+ \nu_e$	$8.97 \pm 0.10$	$(0.00, 2.30)$	$<1.6$	$<209$		

TABLE III: Summary of corrections and systematic uncertainties to  $\mathcal{B}_{\text{SL}}$  in percent (%). A minus sign indicates the MC simulation has higher efficiency than the data.

Source	Correction (%)	Uncertainty (%)
Tracking	-	0.3 - 1.5
$\eta \rightarrow \gamma\gamma$ reconstruction	-6.5	4.0
$\pi^0$ finding	-5.8 - -5.0	2.5 - 3.6
Electron identification	-1.2 - -1.0	1.0
Background shape	-	0.0 - 1.8
Hadron identification	-6.9 - -2.2	0.2 - 0.8
Number of $D$ tags	-	0.5
Veto of unused tracks	-	0.3
Signal Shape	-	0.0 - 0.4
Simulation of form factors	-	1.0 - 3.0
Simulation of FSR	-	0.6
MC statistics	-	0.9 - 1.8
Total	-12.6 - -7.6	3.8 - 4.8